

# Axial intensity of apertured Bessel beams

R. Borghi and M. Santarsiero

*Dipartimento di Fisica, Università La Sapienza, Piazzale Aldo Moro 2, 00185 Rome, Italy*

F. Gori

*Dipartimento di Fisica, Terza Università di Roma, Via della Vasca Navale 84, 00146 Rome, Italy*

Received March 21, 1996; accepted August 2, 1996

We give a simple interpretation of a recently noted phenomenon, namely, the resemblance between the axial intensity of an apertured Bessel beam and the squared profile of the windowing function. We also discuss how this effect can be used to control the axial behavior of the beam, and we present examples for the case of a flattened Gaussian profile as aperturing function. © 1997 Optical Society of America. [S0740-3232(97)02701-4]

Bessel beams,<sup>1-6</sup> or nondiffracting beams, are exact solutions of the scalar Helmholtz equation that maintain the same intensity profile at any plane orthogonal to the propagation direction. They owe their name to the fact that the solution of order  $n$  has a transverse field distribution proportional to the  $n$ th order Bessel function of the first kind,  $J_n$ .<sup>7</sup> Their main feature is that they can transport radiation without any spread or divergence. For this reason, since their introduction Bessel beams have attracted the attention of many scientists, who have proposed a great number of applications.<sup>8-12</sup>

Since finite-aperture optical elements are always present in any practical realization,<sup>13-18</sup> a more realistic model for a Bessel beam has to include the presence, at a certain plane ( $z = 0$ ), of a windowing profile. If this profile is chosen as a Gaussian function, the so-called Bessel-Gauss beams are obtained,<sup>19</sup> whose expression in free paraxial propagation can be given in closed form. When other forms of aperturing profiles are used, the propagated field generally has to be evaluated numerically.<sup>20-22</sup>

It was recently shown that the axial intensity of an apertured Bessel beam of zero order can exhibit some resemblance to the squared profile of the window,<sup>23,24</sup> and this could afford a means to control axial behavior of the beam.

In this paper we give a simple explanation for such a resemblance. This enables us to specify under which conditions the phenomenon occurs, furnishing an operating criterion for controlling the axial intensity of an apertured Bessel beam. To illustrate our main conclusions we shall work out an example, in which a flattened Gaussian (FG) profile<sup>25</sup> is used as a windowing function.

We shall start from the expression of the field at a typical point  $(r, z)$  produced by a Bessel beam of zero order passing through a circularly symmetric window profile  $p(r)$  centered at the beam axis. Assuming that the propagation is in the paraxial regime, such a field, say,  $V(r, z)$ , is<sup>26,27</sup>

$$V(r, z) = -\frac{ikA}{z} \exp\left(ikz + \frac{ik}{2z} r^2\right) \int_0^{+\infty} p(\rho) J_0(\beta\rho) \times J_0\left(\frac{kr\rho}{z}\right) \exp\left(\frac{ik}{2z} \rho^2\right) \rho d\rho, \quad (1)$$

where  $k$  is the wave number,  $A$  is an amplitude factor, and  $\beta$  characterizes the Bessel beam. As is well known, the Bessel field can be thought of as arising from the superposition of plane waves whose wave vectors are evenly distributed on a cone. If we denote by  $\theta$  the semiaperture of the cone, the parameter  $\beta$  is simply given by

$$\beta = k \sin \theta. \quad (2)$$

It follows from Eq. (1) that along the  $z$  axis ( $r = 0$ ) the field is

$$V(0, z) = -\frac{ikA}{z} \exp(ikz) \int_0^{+\infty} p(\rho) J_0(\beta\rho) \times \exp\left(\frac{ik}{2z} \rho^2\right) \rho d\rho, \quad (3)$$

where we took into account that  $J_0(0) = 1$ .

Let us now consider a different situation in which the profile is illuminated by a single plane wave impinging orthogonally on the aperture plane. If we denote by  $A$  the amplitude of the illuminating wave, within the paraxial approximation the new field distribution, say,  $U(r, z)$ , is

$$U(r, z) = -\frac{ikA}{z} \exp\left(ikz + \frac{ik}{2z} r^2\right) \int_0^{+\infty} p(\rho) \times J_0\left(\frac{kr\rho}{z}\right) \exp\left(\frac{ik}{2z} \rho^2\right) \rho d\rho. \quad (4)$$

Comparing Eqs. (3) and (4) and taking Eq. (2) into account, we see that the following relation holds:

$$|V(0, z)|^2 = |U(z \sin \theta, z)|^2. \quad (5)$$

Equation (5) furnishes a simple key for explaining the resemblance phenomenon mentioned above. Indeed, it shows that the axial intensity associated with the apertured Bessel beam is the same as that produced by the sole window (under orthogonal plane-wave illumination) along the line

$$r = z \sin \theta. \quad (6)$$

To explain the resemblance effect, let us begin with the crude representation of Fig. 1(a), where we assume for a moment that the field propagating behind the aperture plane ( $z = 0$ ) can be described by geometrical optics. The gray area schematizes the illuminated region. Starting from the origin  $O$  and moving along the line described by Eq. (6), which is shown in Fig. 1(a) with a dashed line, we would simply see an oblique projection of the window profile. Hence, according to geometrical optics, the axial intensity of the apertured Bessel beam would be equal to the squared profile of the window except for a scale factor  $1/\sin \theta$ , which will be called the geometrical expansion factor. Now let us take diffraction into account. The field distribution behind the aperture will be different from one plane  $z = \text{constant}$  to another instead of being a mere projection of  $p(r)$ . For typical cases the intensity distribution could appear somewhat similar to the rough sketch of Fig. 1(b). When we move along the line of Eq. (6) we can expect the resemblance effect between the axial intensity of the Bessel beam and  $p^2(r)$  to become, generally speaking, weaker and weaker because of the changes introduced by diffraction in the transverse field distribution.

The previous discussion should make it clear that the resemblance effect depends on two main factors. First, if the profile produces considerable diffraction phenomena, the resemblance will be appreciable only in the initial part of the curve representing the axial intensity of the

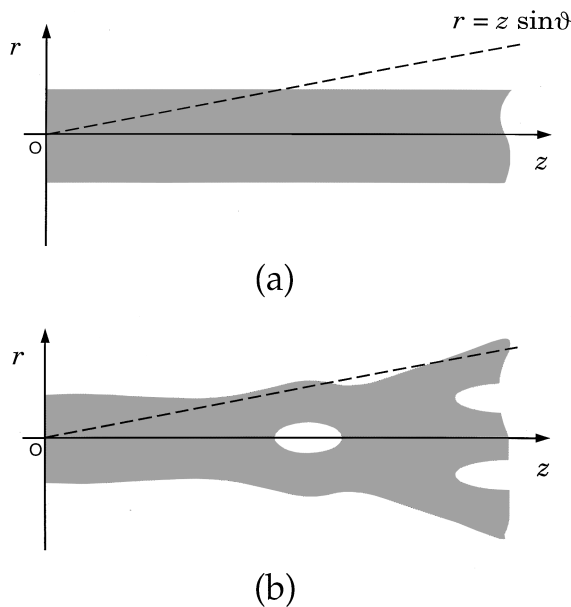


Fig. 1. Representation of the optical intensity behind the window aperture in the case of (a) geometrical approximation and (b) taking into account diffraction effects. The line into Eq. (6) is dashed.

apertured Bessel beam. This is the case, for example, when the profile has a steep descent. On the contrary, slowly varying profiles are likely to enhance the resemblance effect. The second factor is the value of  $\sin \theta$ . For a given profile  $p(r)$  the resemblance effect should increase on increasing  $\sin \theta$ .

FG profiles have recently been introduced<sup>25,28</sup> as an alternative to super-Gaussian windows.<sup>29</sup> Their main property is that the field distribution of a beam possessing a FG profile at its waist (or, briefly, a FG beam) can be evaluated in a simple, closed form at any point in space. The flatness of these profiles is controlled by an integer parameter  $N$ . In particular, for  $N \rightarrow \infty$  the profile tends to the function  $\text{circ}(r/w_0)$ ,<sup>30</sup>  $w_0$  being the width of the profile.<sup>25,28</sup> The key for studying the propagation of the field generated by FG profiles (under orthogonal plane-wave illumination) is the fact that they can be expressed by a finite sum of Laguerre–Gauss functions.<sup>25,26</sup> More explicitly, the FG profile of order  $N$  can be written as

$$p^{(N)}(r) = \sum_{n=0}^N c_n L_n \left[ \frac{2(N+1)r^2}{w_0^2} \right] \exp \left[ -\frac{(N+1)r^2}{w_0^2} \right], \quad (7)$$

where  $L_n$  is the  $n$ th Laguerre polynomial and the expansion coefficients  $c_n$  are given by<sup>25</sup>

$$c_n = (-1)^n \sum_{m=n}^N \binom{m}{n} \frac{1}{2^m}. \quad (8)$$

By using Eq. (5) as well as the formulas describing the propagation of FG beams,<sup>25,28</sup> we can easily find the following expression for the axial intensity, say,  $I_a(z)$ , of the apertured Bessel beam:

$$I_a(z) = \left( \frac{v_0}{v_z} \right)^2 \left| \sum_{n=0}^N c_n \exp[-i(2n+1)\phi_z] \times L_n \left( \frac{2z^2 \sin^2 \theta}{v_z^2} \right) \right|^2 \exp \left( -\frac{2z^2 \sin^2 \theta}{v_z^2} \right), \quad (9)$$

where the following quantities have been introduced:

$$\begin{aligned} v_0 &= w_0 / \sqrt{N+1}, \\ v_z &= v_0 \left[ 1 + \left( \frac{z}{z_R} \right)^2 \right]^{1/2}, \\ \phi_z &= \tan^{-1} \left( \frac{z}{z_R} \right), \\ z_R &= \frac{\pi w_0^2}{\lambda(N+1)}. \end{aligned} \quad (10)$$

It should be noted that, owing to the use of a FG profile as a windowing function, the axial intensity  $I_a$  can be evaluated in a closed form, without any approximations.

To obtain numerical results comparable with those presented in Ref. 24, we studied the behavior of the axial intensity of a Bessel beam with  $\beta = 40 \text{ mm}^{-1}$  apertured by FG profiles having  $w_0 = 4 \text{ mm}$  and with several values of  $N$  [see Eq. (7)]. The wavelength is assumed to be  $\lambda = 632.8 \text{ nm}$ . Figure 2 shows  $I_a(z)$  for  $N = 10, 100, 1000$  and can be compared with Fig. 2 of Ref. 24, where

the axial intensity of the same Bessel beam apertured by different types of windowing functions is shown. As was expected, for small values of  $N$ ,  $I_a$  is a rather smooth function of  $z$ , whereas increasing  $N$  causes ripples to appear and diffraction effects to become more and more evident, as in Fig. 2(a) of Ref. 24, where a circ function was the window profile.

In Fig. 3 the windowing function is a FG profile with  $w_0 = 4$  mm and  $N = 200$ , and curves are shown for different values of  $\beta$  to highlight the fact that, for a given profile, the resemblance effect increases with increasing  $\sin \theta$ , i.e.,  $\beta$  [see Eq. (2)]. In the figure the axial intensity is reported as a function of  $z \sin \theta$ , to compensate the aforementioned geometrical expansion factor  $1/\sin \theta$ . The solid curves correspond to  $\beta = 40$  mm<sup>-1</sup> [curve (a)],  $\beta = 100$  mm<sup>-1</sup> [curve (b)], and  $\beta = 200$  mm<sup>-1</sup> [curve (c)], whereas the dashed curve is the squared window profile itself. It can be noted that, for increasing  $\beta$ , the resemblance effect between the axial intensity and the squared FG profile is more and more evident, as was expected. Furthermore, a qualitative agreement could be observed between our curves and the ones obtained by Cox and

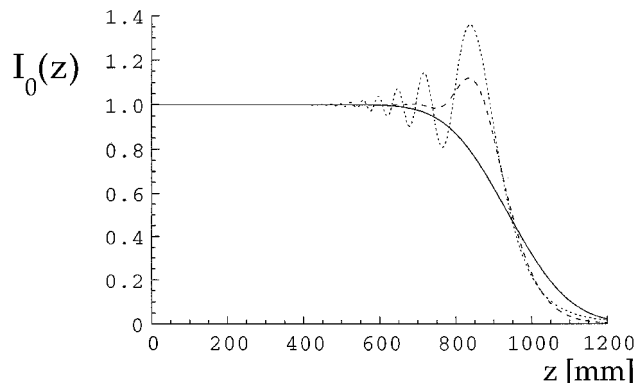


Fig. 2. Behavior of axial intensity  $I_a$  as a function of  $z$  for a Bessel beam with  $\beta = 40$  mm<sup>-1</sup> apertured by a FG profile having spot size  $w_0 = 4$  mm;  $N = 10$  (solid curve), 100 (dashed curve), and 1000 (dotted curve).  $\lambda = 632.8$  nm.

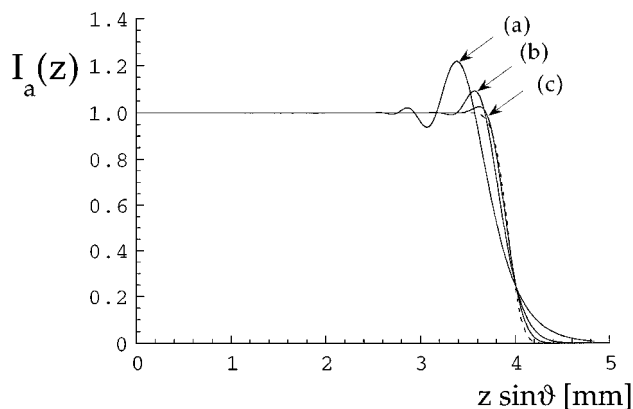


Fig. 3. Axial intensity of a Bessel beam apertured by a FG profile with  $w_0 = 4$  mm and  $N = 200$ , for  $\beta = 40$  mm<sup>-1</sup> [curve (a)],  $\beta = 100$  mm<sup>-1</sup> [curve (b)], and  $\beta = 200$  mm<sup>-1</sup> [curve (c)], as a function of  $z \sin \theta$ . The squared window function is drawn as a dashed line to assess the resemblance effect.

D'Anna,<sup>23</sup> where the axial intensities obtained with a few different flattened profiles were evaluated numerically.

## ACKNOWLEDGMENT

This work is supported by Ministero dell'Università e della Ricerca Scientifica e Tecnologica and Istituto Nazionale di Fisica della Materia.

## REFERENCES AND NOTES

1. C. J. R. Sheppard and T. Wilson, "Gaussian-beam theory of lenses with annular aperture," *Microwaves Opt. Acoust.* **2**, 105–112 (1978).
2. J. Durnin, J. Miceli, Jr., and J. H. Eberly, "Diffraction-free beams," *Phys. Rev. Lett.* **58**, 1499–1501 (1987).
3. J. Durnin, "Exact solutions for nondiffracting beams. I. The scalar theory," *J. Opt. Soc. Am. A* **4**, 651–654 (1987).
4. G. Indebetouw, "Nondiffracting optical field: some remarks on their analysis and synthesis," *J. Opt. Soc. Am. A* **6**, 150–152 (1989).
5. P. Szwaykowski and J. Ojeda-Castañeda, "Nondiffracting beams and self-imaging phenomena" *Opt. Commun.* **83**, 1–4 (1991).
6. Z. Bouchal and M. Olivik, "Non-diffractive vector Bessel beams," *J. Mod. Opt.* **42**, 1555 (1995).
7. M. Abramowitz and I. Stegun, *Handbook of Mathematical Functions* (Dover, New York, 1972).
8. J. K. Jabczynski, "A diffraction-free resonator," *Opt. Commun.* **77**, 292–294 (1990).
9. J. Lu, X. Xu, H. Zou, and J. F. Greenleaf, "Application of Bessel beams for Doppler velocity estimation," *IEEE Trans. Ultrason. Ferroelec. Freq. Control* **42**, 649–662 (1995).
10. K. M. Iftekharuddin and M. A. Karim, "Heterodyne detection by using a diffraction-free beam: tilt and offset effect," *Appl. Opt.* **31**, 4853–4856 (1992).
11. R. P. Macdonald, J. Chrostowski, S. A. Boothroyd, and B. A. Syrett, "Holographic formation of a diode laser nondiffracting beam," *Appl. Opt.* **32**, 6470 (1993).
12. S. Klewitz, F. Brinkmann, S. Herminghaus, and P. Leiderer, "Bessel-beam-pumped tunable distributed feedback laser," *Appl. Opt.* **34**, 7670–7673 (1995).
13. J. Turunen, A. Vasara, and A. T. Friberg, "Holographic generation of diffraction-free beams," *Appl. Opt.* **27**, 3959–3962 (1988).
14. A. Vasara, J. Turunen, and A. T. Friberg, "Realization of general nondiffracting beams with computer-generated holograms," *J. Opt. Soc. Am. A* **6**, 1748–1754 (1989).
15. R. M. Herman and T. A. Wiggins, "Production and uses of diffractionless beams," *J. Opt. Soc. Am. A* **8**, 932–942 (1991).
16. K. Thewes, M. A. Karim, and A. A. S. Awwal, "Diffraction-free beam generation using refracting system," *Opt. Laser Technol.* **23**, 105–108 (1991).
17. G. Scott and M. McArdle, "Efficient generation of nearly diffraction-free beams using an axicon," *Opt. Eng.* **31**, 2640–2643 (1992).
18. N. Davidson, A. A. Friesem, and E. Hasman, "Efficient formation of nondiffracting beams with uniform intensity along the propagation direction," *Opt. Commun.* **88**, 326–330 (1992).
19. F. Gori, G. Guattari, and C. Padovani, "Bessel-Gauss beams," *Opt. Commun.* **64**, 491–495 (1987).
20. L. Vicari, "Truncation of non-diffracting beams," *Opt. Commun.* **70**, 263–266 (1989).
21. S. De Nicola, "Irradiance from an aperture with a truncated  $J_0$  Bessel beam," *Opt. Commun.* **80**, 299–302 (1991).
22. P. L. Overfelt and C. S. Kenney, "Comparison of the propagation characteristic of Bessel, Bessel-Gauss, and Gaussian beams diffracted by circular apertures," *J. Opt. Soc. Am. A* **8**, 732–745 (1991).

23. A. J. Cox and J. D'Anna, "Constant-axial-intensity nondiffracting beam," *Opt. Lett.* **17**, 232–234 (1992).
24. Z. Jiang, Q. Lu, and Z. Liu, "Propagation of apertured Bessel beams," *Appl. Opt.* **34**, 7183–7185 (1995).
25. F. Gori, "Flattened Gaussian beams," *Opt. Commun.* **107**, 335–341 (1994).
26. A. E. Siegman, *Lasers* (University Science, Mill Valley, Calif., 1986), Chap. 16.
27. L. Mandel and E. Wolf, *Optical Coherence and Quantum Optics* (Cambridge U. Press, Cambridge, 1995).
28. V. Bagini, R. Borghi, F. Gori, A. M. Pacileo, M. Santarsiero, D. Ambrosini, and G. Schirripa Spagnolo, "Propagation of axially symmetric flattened Gaussian beams," *J. Opt. Soc. Am. A* **13**, 1385–1394 (1996).
29. S. De Silvestri, P. Laporta, V. Magni, and O. Svelto, "Solid-state laser unstable resonators with tapered reflectivity mirrors: the super-Gaussian approach," *IEEE J. Quantum Electron.* **24**, 1172–1177 (1988).
30. As usual,  $\text{circ}(r)$  is defined as 1 if  $r \leq 1$  and 0 elsewhere,  $r$  being the radial coordinate in  $R^2$ .